The Kosterlitz-Thouless phase transition and the XY model

Anushka Menon, Arsalan Ahmad Chattha, and Yashasvee Goel
(Dated: February 26, 2023)

In this report, we talk about the XY Model which is the generalization of the 2D Ising Model. Firstly, we look at the Hamiltonian to study the nearest neighbour couplings and simulate it using the Hamiltonian Monte Carlo (HMC) algorithm. We see the dependence of magnetization and susceptibility on temperature and observe that it exhibits phase transition at the critical temperature. The phase transition exhibits interesting behaviour where the system transitions from disordered high-temperature state to a quasi-ordered state below some critical temperature which is called the Kosterlitz-Thouless transition.

I. INTRODUCTION

In this report, we study the XY Model and its phase transitions and simulate them using the HMC algorithm with the help of `python`. The two-dimensional XY model is a system of spins constrained to rotate in the plane of the lattice which, for simplicity, we take to be a simple square lattice. We have a system with 2-dimensional continuous spin vectors $\vec{s} = (\vec{s_x}, \vec{s_y})$ of a fixed unit norm $\vec{s^2} = {s_x}^1 + {s_y}^2 = 1$ and a Hamiltonian [1][7]:

$$\mathcal{H}(\vec{J}) = -J \sum_{<i,j>} \vec{s_i}.\vec{s_j} \tag{1}$$

where the summation runs over the nearest neighbouring sites.

The motivation for the XY model can be summarized as follows. Firstly, the model is useful in helping us understand all sorts of behaviour under phase transition and interpret changes in the system around the critical temperatures. Secondly, the model can be used to compute thermodynamic quantities and interpret them. Various thermodynamic quantities such as magnetization, energy, susceptibility, etc. can be studied for a range of temperatures. Lastly, it's a simple model that can be applied to a number of systems such as films of super fluid helium, superconducting materials, fluctuating surfaces, Josephson-junctions as well as certain magnetic, gaseous and liquid-crystal systems [6].

The phase transition exhibited by the model is unique. When the system transitions from disordered high-temperature state to a quasi-ordered state below some critical temperature, it is called the Kosterlitz-Thouless transition. In this case, vortex generation becomes thermodynamically possible when we are at the critical temperature T_c.

In this report, we will study the XY model of ferromagnetism for values above and below the critical temperature. In Sec.II, we will discuss the underlying theory for the model where we will learn about the characteristics of the model. We will also look into the various thermodynamic quantities like Magnetization, Susceptibility, etc. in detail. In Sec.III, we talk about the methods, where the working of the respective algorithms and simulations are discussed. In Sec.IV, we will discuss the results. Here, we will interpret the trends of various thermodynamic quantities with respect to temperature. Lastly, we will obtain the value of critical temperature from the code and compare it to the theoretical value. Finally, we summarize our work in Sec.V.

II. THEORETICAL BASIS

We start by learning about the Hamiltonian of our model which is defined in Eq.(1). Consider a 2-D simple square lattice Λ. Here J is the coupling constant (we study for $J > 0$, here we study the ferromagnetic case), s_i and s_j are the spins where i label indicates the i^{th} site on the lattice and j is its corresponding neighbour. The spin configuration is defined as $\vec{s} = (\vec{s_x}, \vec{s_y})$ which can be written in terms of angle as $s_j = (\cos\theta_j, \sin\theta_j)$, where $-\pi < \theta_j < \pi$ for all j in Λ. We can then write our Hamiltonian in the form of [7]:

$$\mathcal{H}(\vec{J}) = -J \sum_{<ij>} \cos(\phi_i - \phi_j) \tag{2}$$

This model is an example of a 2-dimensional model with continuous symmetry which does not have long-range order.The probability of each state to occur is given by [5]:

$$P = \frac{1}{Z} \exp(\frac{-E}{k_B T}) \tag{3}$$

here $\beta = \frac{1}{k_B T}$ where T is the temperature, k_B is the Boltzmann constant and E is the energy. The

partition sum Z for a temperature T can be given as [1]:

$$Z = \sum_{\vec{s}} \exp(\frac{-\mathcal{H}}{k_B T}) \tag{4}$$

A. Mermin-Wagner theorem

The Mermin-Wagner theorem states that at finite temperatures continuous symmetry cannot be broken for one or two dimensional theories for sufficiently short-range interaction systems [4]. This essentially tells us that for such symmetries the ordered parameters can have expectation values only for the ground-state i.e. when $T = 0$ exactly. As the dimensions are lowered, the fluctuations become more dominant upto the point of destroying any potential ordering below critical dimensions. This theorem is widely applicable which include their application for magnet, solids and super-fluids.

The XY model doesn't exhibit the conventional long-range order as the Ising model. This is due to the instability of its ground state against the spin wave excitations for low-energy. This was first shown by Mermin and Wagner in 1966 [10].

There is no symmetry breaking for phase transitions rather the system does show signs of a transition from a disordered state to a quasi-ordered state below some critical temperature known as the Kosterlitz-Thouless transition.

The correlation between two spins are given by vortex configurations (which we will discuss later in II E) and spin wave excitations. By ignoring the vortex configuration, we get the spin-wave correlation function as follows [8]:

$$\langle S_i.S_j \rangle = \langle exp(i(\phi_i - \phi_j)) \rangle \tag{5}$$

Simplifying above expression gives the form:

$$\langle S_i S_j \rangle \approx |\frac{r_i - r_j}{r_0}|^{\frac{-k_B T}{4\pi J}} \tag{6}$$

for $|r_i - r_j| >> a$, where r_0 is a cutoff of the order of the lattice spacing 'a'. Thus, we see that the spin-wave excitations are responsible in destroying the long-range order in the system.

B. Magnetization

Using Monte-Carlo simulations with Metropolis algorithm, various thermodynamic properties of the XY model can be computed for a range of temperatures. This includes the mean magnetization per site of the system. The mean magnetization per site is nothing but the net magnetic moment of the system at each site. The magnetization in the XY model is found to be zero in the thermodynamic limit. However, macroscopic magnetization can be observed for a finite system at lower temperatures. This shows that there are spin spaces in the lattice that align themselves to give a net non-zero magnetization. For higher temperatures the component of spins are randomized and hence the magnetization slowly goes on decreasing tending to zero [9].

$$M = \frac{1}{N} |\langle (\Sigma_{i=1}^{N} \cos\theta_i, \Sigma_{i=1}^{N} \sin\theta_i) \rangle| \tag{7}$$

This transition of magnetization with temperature helps us study the phase transition in the model which does not occur in a thermodynamic limit.

C. Susceptibility

Along with magnetization, susceptibility is another thermodynamic quantity which helps us understand the phase transition in the XY model. Susceptibility can be written in terms of variance of magnetization as follows [9]:

$$\chi = \frac{1}{NT} (\langle |M|^2 \rangle - \langle |M| \rangle^2) \tag{8}$$

The susceptibility has small change for lower range of temperatures and has a sudden growth around the Kosterlitz-Thouless critical temperature T_C. This behaviour is similar to a delta function where at lower temperatures, spins align themselves by pointing in the same direction. However, as we reach around the transition temperature, a dramatic increase of random oriented spins result in shoot in the susceptibility value.

D. Specific Heat

Using these thermodynamic quantities, we can also calculate specific heat of the system. The specific heat is calculated based on the mean square fluctuations of the total energy E as [11]:

$$c = \frac{1}{NT^2} (\langle E^2 \rangle - \langle E \rangle^2) \tag{9}$$

Unlike other thermodynamic quantities, where transition of phase is seen around the critical temperature, the specific heat doesn't show divergence at critical temperature. Instead, the specific heat is found to have a peak at $1.167(1)k_BT/J$.

E. Phase Transition

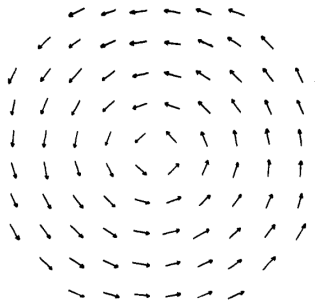

FIG. 1: Isolated vortex for the XY model. [8]

In the 2-dimensional XY model, phase transition is seen from a disordered state at high temperatures to quasi-ordered state below critical temperatures. This is known as Berezinskii–Kosterlitz–Thouless transition (BKT transition) which led to a Nobel prize in Physics in 2016 being awarded to Thouless and Kosterlitz.

The topological defects of the model can also be explained in terms of unbinding of vortices from low temperature phase to disordered high temperature phase. Vortices are flux circulation of some physical quantity. The formation of vortices are preferred at high temperatures above the critical temperature T_c as the entropy term takes over. For lower temperatures, the energy term dominates and makes it unfavourable for isolated vortices to occur shown in Fig. 1. The critical temperature at which phase transition is observed can be given as [7]:

$$T_C \approx \frac{\pi J}{k_B} \tag{10}$$

Correlation is an important quantity in studying the phase transition of the XY model. Vortex configurations and spin wave excitations gives the correlation between two neighbouring spins. The correlation length has an exponential curve for higher temperatures and for temperatures below the critical temperature it has a power law. Below the critical temperature, the vortices favour to be bound together in close pairs of zero vorticity. The effect of a close pair on some spin distant from it is negligible since they almost cancel out each other. The mean separation for such small pairs of vortices are found to be finite even as we approach the critical temperature. Above the critical temperature, under the influence of arbitrary weak external magnetic field, the vortices are free to move to the surface in response to this applied field.

III. METHOD

A. Artificial Hamiltonian

As we saw in the lectures, we begin by defining an artificial Hamiltonian for the system. The general form of the same is:

$$\mathcal{H}_{artificial} = \frac{1}{2}\sum_i p_i^2 + \mathcal{S}[\phi] \tag{11}$$

where p_i is the conjugate momenta and $\mathcal{S}$ is the action. Hence, for our model, the artificial Hamiltonian comes out to be:

$$\mathcal{H}_{artificial} = \frac{1}{2}\sum_i p_i^2 - \beta J \sum_{<ij>} \cos(\phi_i - \phi_j) \tag{12}$$

We use this Hamiltonian to calculate the equations of motion in the next section.

B. Leapfrog Integrator

Leapfrog integrator is a method for numerically integrating differential equations. The equations of motion for out Hamiltonian are as follows:

$$\dot{p} = -J \sum_{<ij>} \sin(\phi_i - \phi_j) \tag{13}$$

$$\dot{\phi} = p \tag{14}$$

After obtaining the EoM's, we have to integrate them to see the evolution from a point (p_o, ϕ_o) to (p_f, ϕ_f). We use the Leapfrog Integrator to do the same. As we saw in the lectures, this technique is elegantly simple and requires number of function evaluations per step.

Now, we apply the leapfrog algorithm on these equations. To do that, we first define a variable ϵ, where, $\epsilon = 1/N_{md}$ and N_{md} is the number of steps in integration. Then we evolve these two equations with

the respective algorithm. Firstly, we initialize our variables by setting $(p, \Phi) = (p_o, \phi_o)$. The first half step of leapfrog goes as:

$$\Phi = \Phi + \frac{\epsilon}{2} p \tag{15}$$

After taking the half step, we repeat the process $N_{md} - 1$ times by using the equations of motion as:

$$p = p + \epsilon(-J \sum_{<ij>} \sin(\phi_i - \phi_j))$$

$$\Phi = \Phi + \epsilon p$$

For the last step, we have to take half step back and so we use:

$$p = p + \epsilon(-J \sum_{<ij>} \sin(\phi_i - \phi_j))$$

$$\Phi = \Phi + \frac{\epsilon}{2} p$$

In the end, we get the evolved quantities and we set them as $(p, \Phi) = (p_f, \phi_f)$. Hence, we have a working integrator and we can check the correctness of our code by plotting its convergence. To do that we take the difference between the initial and final Hamiltonian values. The graph is plotted between $\frac{|H_f - H_o|}{H_o}$ v/s N_{md}. We will end this section with a discussion of the importance of leapfrog integrator.

- Time reversibility: We can integrate, say, n steps forward and then simply reverse the direction of integration to reach the same position.
- Nature: It has a symplectic nature which sometimes allows the conservation of energy.

Because of these two reasons, this integrator can be used in Hamiltonian Monte Carlo method which is discussed in the next section.

C. Hamiltonian Monte Carlo Algorithm

We start by talking about the working of Hamiltonian Monte Carlo algorithm. In this, we aim on obtaining a sequence of random samples, i.e. Markov chain, from a probability density. We will now look at the implementation of the algorithm step by step [2].

- **Sampling:** In the first step, the new values for momentum are randomly chosen from their Gaussian distribution.
- **Leapfrog Integrator:** The integrator then operates on this particular distribution by drawing a fresh momentum term independently of previous momentum value.
- **Metropolis Accept-Reject:** To account for numerical errors during the integration, we apply the Metropolis acceptance step. Here the probability to keep the new value, say, p' changing from p, depends $min(1, \exp^{(\mathcal{H}(p,\phi) - \mathcal{H}(p',\phi'))})$ If the proposal is not accepted, we store ϕ regardless. This helps us in generating a whole chain of ϕ' s which is in turn our Markov chain.

Here, we also check the acceptance rate of the algorithm to ensure that is atleast more than 60%. In summary, the Hamiltonian Monte Carlo algorithm starts at a specified initial set of parameters ϕ. Then, for a given number of iterations, a new momentum vector is sampled and the current value of the parameter ϕ is updated using the leapfrog integrator with number of steps N_{md} and ϵ. Then a Metropolis acceptance step is applied, and a decision is made whether to update to the new state (ϕ', p') or keep the existing state.

D. Error Estimation

We calculate errors for our simulation using a method called the Bootstrap error estimation. This method allows estimation of sampling distribution of a statistic using random sampling methods. It is famously using in sampling population databases. The basic idea of bootstrapping is that it re-samples a single data set to create many simulated samples. One of the advantages to use this method is its simplicity. We can straight away derive estimated standard errors for complex distributions because we do not need to *measure* the data set again.
A general process of bootstrap is as follows:

- Statistic of interest: $s(x)$
- A random observed sample: $x = (x_1, x_2, x_3, ..., x_n)$
- Bootstrap sample: $x^* = ({x_1}^*, {x_2}^*, {x_3}^*, ..., {x_n}^*)$
- Boostrap replicates: $s(x^*) = (s({x_1}^*), s({x_2}^*), s({x_3}^*), ..., s({x_n}^*))$

- Bootstrap standard error: $\hat{se}_{boot}$

We applied this method to obtain the errors for all the thermodynamic quantities. After obtaining the arrays for Energy and Magnetization, we binned them and generated their bootstrap samples. Each of these simulated samples has its own properties, such as the mean. Then we measure their standard deviation which gives us the error and plot them simultaneously with the thermodynamic quantity. The code for the same was integrated in the HMC algorithm with the help of our tutor. This helped in optimizing the code and faster computation. The estimated error for the respective thermodynamic quantity can be seen in the plots given in Sec.IV.

IV. RESULTS

The very first thing we check on our code is the convergence of the Leapfrog Integrator III B. The following is the plot obtained by our code:

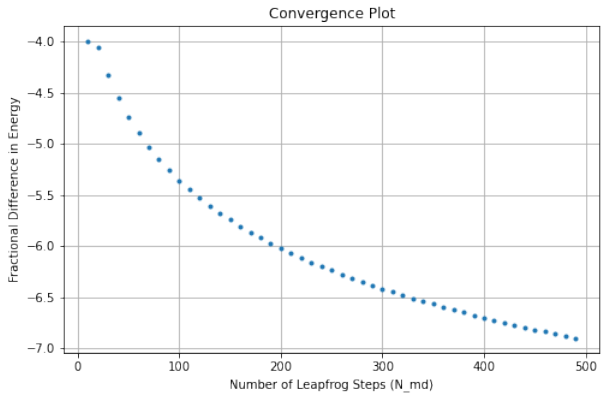

FIG. 2: Convergence of Leapfrog Integrator for the code

The quantity on y-axis is the fractional difference in the energy which is given by $\frac{|H_f - H_o|}{H_o}$ and the quantity on x-axis is the number of Leapfrog steps, N_{md}. We see that the plot converges which is a check to indicate the quality of the integrator. Now, we can use this to implement the famous HMC algorithm in the code.
We discussed the steps of HMC in Sec.III C. When we apply the same in our code, our aim is mainly at two quantities, *Magnetization* (m), and, *Energy* (E). The output of this algorithm gives us two arrays respectively, which we then use to calculate other quantities such as Susceptibility and Specific Heat.

A. Temperature Dependence of Magnetization

We discussed in Sec.II B, the dependence of magnetization on temperature. As mentioned earlier, the HMC gives us two arrays where one of them is the Magnetization array. Taking mean of this array and plotting it for a range of of temperatures $(T = [0.1, 2.20]K)$ in step size of 0.20, gives us the plot in Figure 3. This is a plot for various value of N specifically, $N = 5, 8, 10, 12, 15$, where the size of the lattice is $N \times N$.

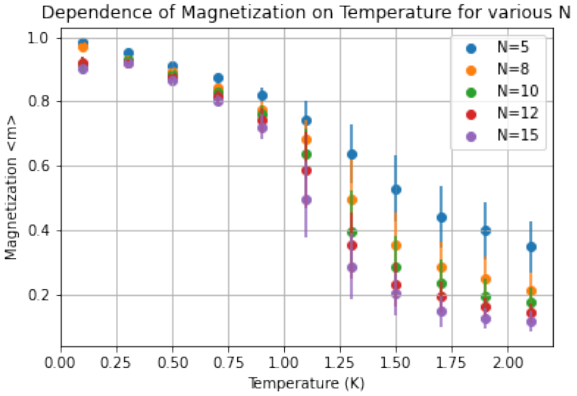

FIG. 3: Dependence of Magnetization on Temperature for various lattice sizes (N × N)

We see that the mean magnetization goes on decreasing with increase in the value of T. This is because at lower value of temperatures (T) the spins spaces tend to align themselves to give a net magnetization. However, in high temperature regions the angles are randomly distributed in space and magnetization vanishes slowly. This change is given by a slowly decreasing exponential curve where transition can be seen to occur at critical temperature T_C. Although, the decrease with system size is not very prominent, we see that magnetization is smaller for lattices with larger size and this difference becomes prominent at higher values of temperatures. This is because larger lattice size contains more randomized spin configurations at higher temperatures resulting in vanishing magnetization. The critical temperature is also found to drop steeply for larger lattice size.

B. Temperature Dependence of Energy

Next, we plot the mean of the Energy array which contains the energy values against the same values of

T. Here, we see the mean energy per site slowly goes on increasing with temperature and is maximum for largest temperature.

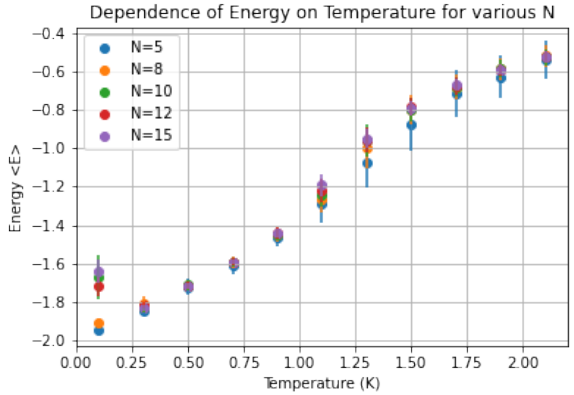

FIG. 4: Dependence of Energy on Temperature for various lattice sizes (N × N)

At lower temperatures, the linear regime where angles between neighbouring spins are small is observed. But, as temperature goes on increasing, the contribution from potential energy becomes negligible resulting in increase in free spins in the lattice. This change in the behaviour of the curve happens around the critical temperature T_C. The energy dependence was observed to have same curve for all lattice sizes.

C. Temperature Dependence of Susceptibility

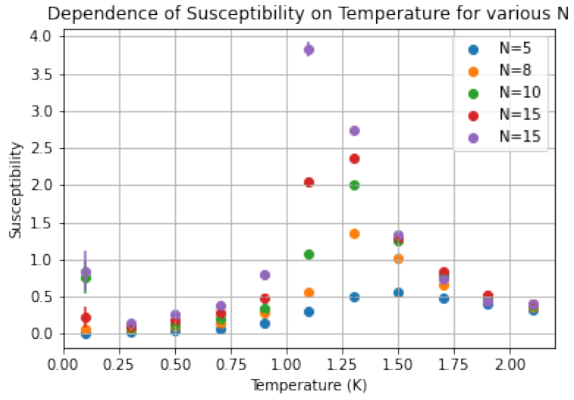

FIG. 5: Dependence of Susceptibility on Temperature for various lattice sizes (N × N)

The susceptibility is related to the variance of magnetization as given in Eq.(8). We can therefore find susceptibility with the help of the magnetization values used to plot Fig. 3. In Fig. 6 we see that the curve is similar to a delta function curve, where the susceptibility gives a small value for lower and higher values of temperatures. However, we see a sharp peak for critical temperatures indicating phase transition of the system. This is due to the fact that around these temperatures, the amount of randomly oriented spins increase dramatically . We can also infer from the figure that the peaks are sharper for large values of N. This indicates, larger the size of lattice, more spins are randomized at critical temperatures such that the system becomes highly susceptible.

Note: We defined a variable N_{cfg} in the code, which is the number of configurations for one lattice simulation. When the code ran for $N_{cfg} = 500$, we saw that the fluctuations which are there for the initial value of temperature was absent and the plots were more accurate. However, the plots here are for $N_{cfg} = 200$, due to computational constraint. It is the same case for the plots for Specific Heat.

D. Temperature dependence of Specific Heat

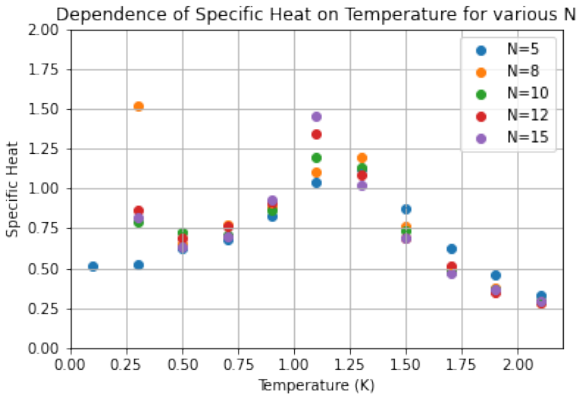

FIG. 6: Dependence of Specific Heat on Temperature for various lattice size (N × N)

Specific heat is given by the variance of energy as described in Eq.(9). Similar to finding susceptibility from magnetization array, we find the specific heat values using the energy array obtained using HMC algorithm.

In Fig.(6), we see a curve with a peak around critical temperature and tails for temperatures below

and above critical temperature. The peak value is found to be sensitive of lattice size with critical temperature being shifted depending on the value of N.

E. Phase Transition and Critical Temperature

After obtaining the plots for Susceptibility and Specific heat for various lattice sizes, we fitted them individually to find the value of Critical Temperature (T_c), for each simulation. To fit the plots, we used the Lorentzian function and `lmfit` module and `scipy` module in `python`. The fitted plots for susceptibility can be referred in Appendix A and for specific heat in Appendix B. The plot for the values of critical temperature obtained from the fitted susceptibility plots is as follows:

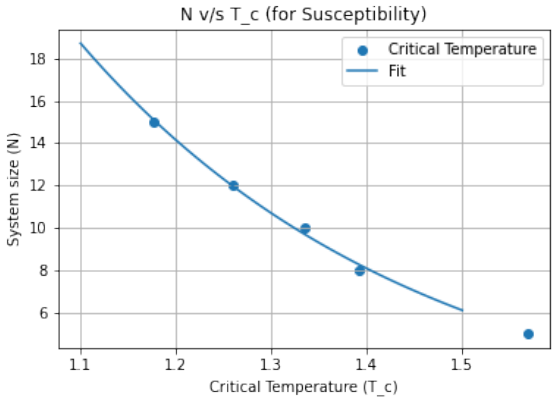

FIG. 7: Trend of Critical Temperature with respect to Lattice size

The critical temperature is on $x-$axis whereas lattice size is on the $y-$axis. We observe that T_c decreases with increasing lattice size. We have fitted an exponential function to check where it diverges and hence, obtain the critical temperature for the infinite system. The value comes out to be $T \approx 1.143\ K$
Next, the plot for the values of critical temperature obtained from the fitted specific heat plots is as follows:

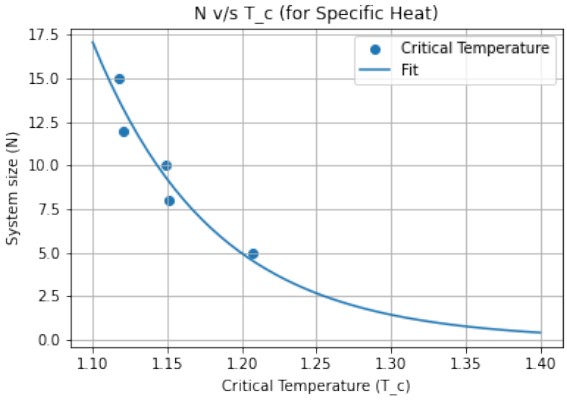

FIG. 8: Trend of Critical Temperature with respect to Lattice size

Again, the critical temperature is on $x-$axis whereas lattice size is on the $y-$axis. The trend is similar to that of Fig.(7) but here we see that the values are very close to each other. The value for critical temperature obtained for the infinite system from this Fig.(8) is $T \approx 1.159\ K$. The theoretical value [3] for the critical temperature for infinite system is $T = 0.893\ K$. We see that the simulated value is higher than the theoretical value. One of the possible reasons for that could be the low number of configurations simulated. Another possible reason could be the quality and nature of the fit function.

V. SUMMARY

In this project, we studied the statistical properties of a 2-dimensional XY model by applying the Hamiltonian Monte-Carlo method with the Metropolis algorithm. We investigated the temperature dependence on Magnetization, Energy, Susceptibility and Specific Heat. There we found phase transition at the Kosterlitz-Thouless critical temperature.

We found the magnetization per site to decrease with temperature and the energy per site to increase with temperature. The magnetization and energy per site were calculated by finding the mean of the arrays computed using HMC with the Metropolis algorithm. The transition is a smooth phase transition which helped us interpret their behaviour around the critical temperature. Thereafter, we plotted and studied the curves for susceptibility and specific heat which gave sharp peaks around the critical temperature. The lattice size played an important role in

shifting the value of critical temperatures for these two thermodynamic quantities.

We then fitted the plots for Susceptibility and Specific heat using a Lorentzian function to obtain the value of T_c. We obtained five values, each, of T_c for Susceptibility and Specific Heat. We study the trend of Critical temperature with increasing lattice size. After that, we fit the two plots using a negative exponential function to obtain the value of critical temperature for infinite system. The value obtained by the Specific heat plot is $T \approx 1.159\ K$ and by the Susceptibility plot is $T \approx 1.143\ K$ We compare this value with the theoretical value of the same which is $T = 0.893\ K$. We see that the simulated value is higher than the theoretical value. One of the possible reasons for that could be the low number of configurations simulated. Another possible reason could be the quality and nature of the fit function (exponential, polynomial, etc.).
We can increase the simulation time to get better results. In extension to the project, we can study the signals of phase transition where we can observe vortices.

VI. ACKNOWLEDGEMENTS

We would like to thank the professors Stefan Krieg, Thomas Luu and Evan Berkowitz for the course. We are also extremely grateful to our tutor Ms. Kriti Baweja for her guidance and support throughout the project.

[1] The beginners guide to hamiltonian monte carlo. "`https://bayesianbrad.github.io/posts/2019_hmc.html`".

[2] The beginners guide to hamiltonian monte carlo. "`https://bayesianbrad.github.io/posts/2019_hmc.html`".

[3] Comparison of exact and numerical results in the xy model. "`https://edoc.hu-berlin.de/bitstream/handle/18452/14664/Korzec.pdf?sequence=1`".

[4] Concepts in condensed matter physics: Tutorial iii, the mermin-wagner theorem. "`https://www.weizmann.ac.il/condmat/oreg/sites/condmat.oreg/files/uploads/2021/mermin_wagner_tutorial.pdf`".

[5] Projects for computational physics: The kosterlitz-thouless phase transition and the xy model. "`https://fz-juelich.sciebo.de/s/16SNCiLjJT2CnFo#pdfviewer`".

[6] Ralph Kenna. The xy model and the berezinskii-kosterlitz-thouless phase transition. *arXiv preprint cond-mat/0512356*, 2005.

[7] JM Kosterlitz. The critical properties of the two-dimensional xy model. *Journal of Physics C: Solid State Physics*, 7(6):1046, 1974.

[8] John Michael Kosterlitz and David James Thouless. Ordering, metastability and phase transitions in two-dimensional systems. In *Basic Notions Of Condensed Matter Physics*, pages 493–515. CRC Press, 2018.

[9] Xavier Leoncini, Alberto D Verga, and Stefano Ruffo. Hamiltonian dynamics and the phase transition of the xy model. *Physical Review E*, 57(6):6377, 1998.

[10] N David Mermin and Herbert Wagner. Absence of ferromagnetism or antiferromagnetism in one-or two-dimensional isotropic heisenberg models. *Physical Review Letters*, 17(22):1133, 1966.

[11] Phong H Nguyen and Massimo Boninsegni. Superfluid transition and specific heat of the 2d x-y model: Monte carlo simulation. *Applied Sciences*, 11(11):4931, 2021.

A. FITTED PLOTS FOR T_c FOR SUSCEPTIBILITY FOR ALL N

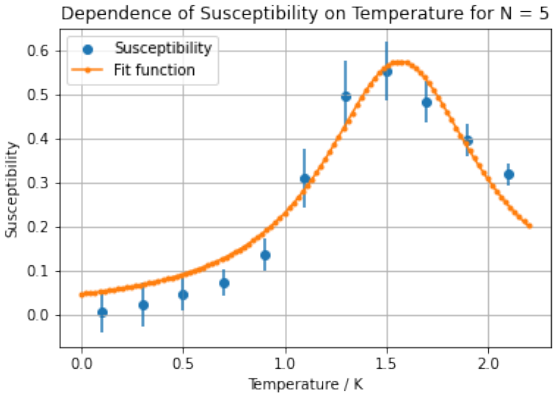

FIG. 9: Dependence of Susceptibility on Temperature for N=5 ($T_c = 1.568\ K$)

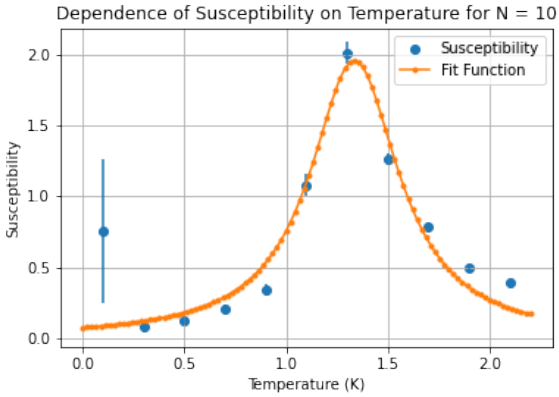

FIG. 11: Dependence of Susceptibility on Temperature for N=10 ($T_c = 1.335\ K$)

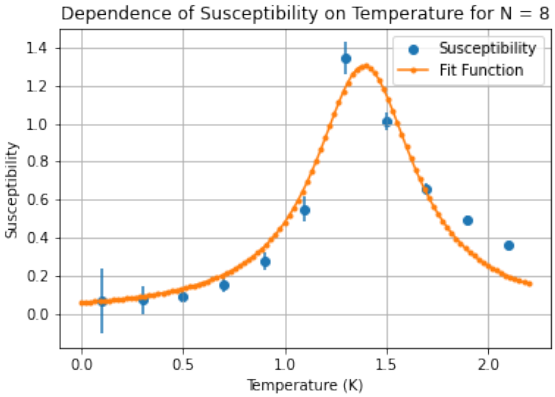

FIG. 10: Dependence of Susceptibility on Temperature for N=8 ($T_c = 1.391\ K$)

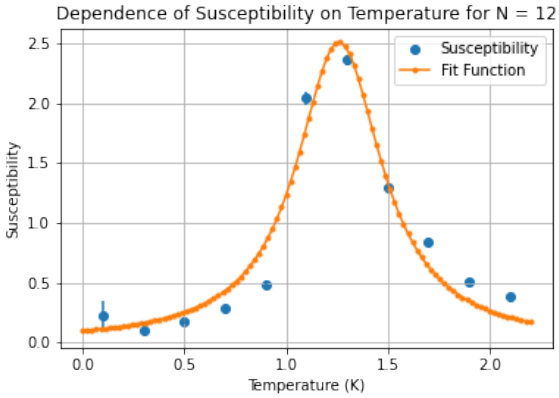

FIG. 12: Dependence of Susceptibility on Temperature for N=12 ($T_c = 1.260\ K$)

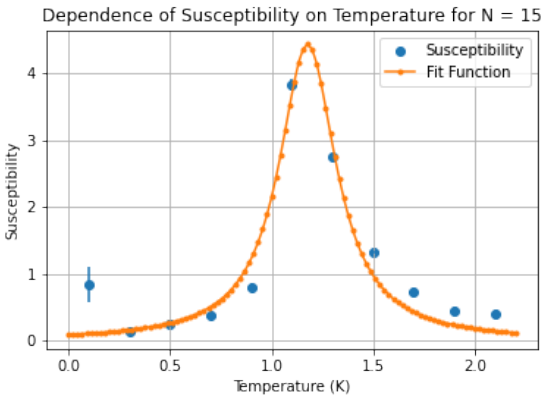

FIG. 13: Dependence of Susceptibility on Temperature for N=15 ($T_c = 1.176\ K$)

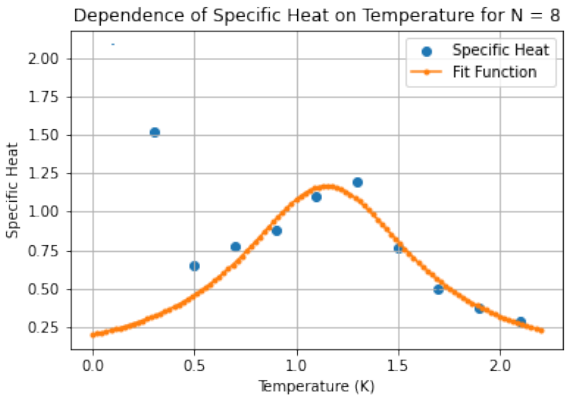

FIG. 15: Dependence of Specific Heat on Temperature for N=8 ($T_c = 1.150\ K$)

B. FITTED PLOTS FOR T_c FOR SPECIFIC HEAT FOR ALL N

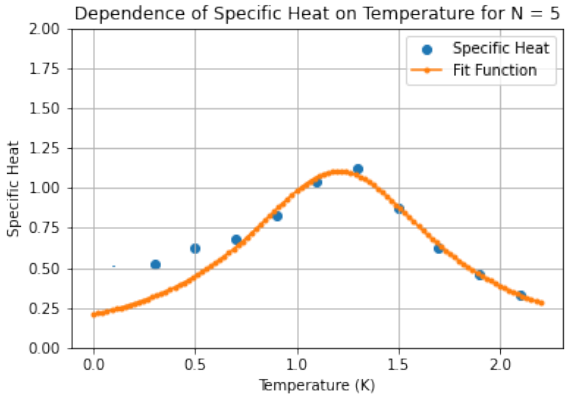

FIG. 14: Dependence of Specific Heat on Temperature for N=5 ($T_c = 1.207\ K$)

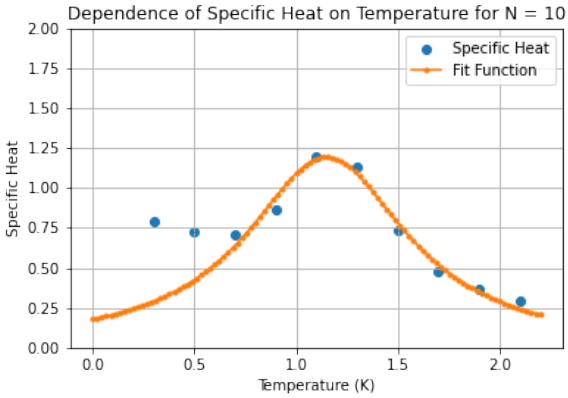

FIG. 16: Dependence of Specific Heat on Temperature for N=10 ($T_c = 1.148\ K$)

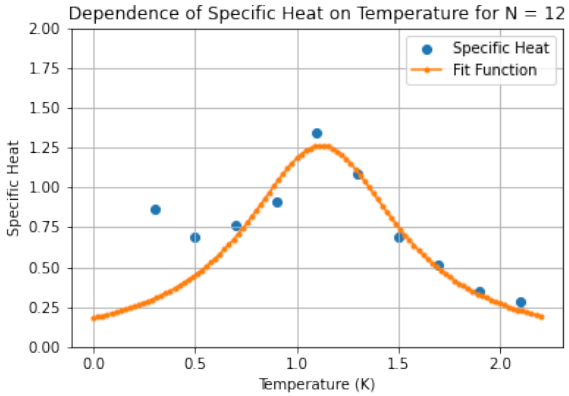

FIG. 17: Dependence of Specific Heat on Temperature for N=12 ($T_c = 1.120\ K$)

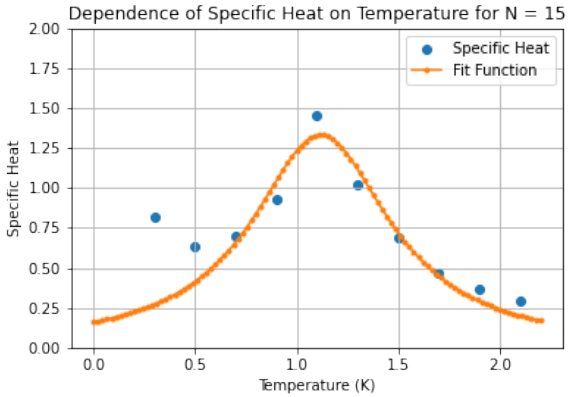

FIG. 18: Dependence of Specific Heat on Temperature for N=15 ($T_c = 1.117\ K$)